



UNIVERSITY OF LEEDS

This is a repository copy of *Rates of carbonate cementation associated with sulphate reduction in DSDP/ODP sediments: implications for the formation of concretions* .

White Rose Research Online URL for this paper:  
<http://eprints.whiterose.ac.uk/404/>

---

**Article:**

Raiswell, R. and Fisher, Q.J. (2004) Rates of carbonate cementation associated with sulphate reduction in DSDP/ODP sediments: implications for the formation of concretions. *Chemical Geology*, 211 (1-2). pp. 71-85. ISSN 0009-2541

<https://doi.org/10.1016/j.chemgeo.2004.06.020>

---

**Reuse**

See Attached

**Takedown**

If you consider content in White Rose Research Online to be in breach of UK law, please notify us by emailing [eprints@whiterose.ac.uk](mailto:eprints@whiterose.ac.uk) including the URL of the record and the reason for the withdrawal request.



[eprints@whiterose.ac.uk](mailto:eprints@whiterose.ac.uk)  
<https://eprints.whiterose.ac.uk/>

**Rates of carbonate cementation associated with sulphate reduction in DSDP/ODP sediments:  
Implications for the formation of concretions**

By R. Raiswell\* and Q.J. Fisher (*School of Earth Sciences, University of Leeds, Leeds LS2 9JT*)

\* Corresponding author; email [r.raiswell@earth.leeds.ac.uk](mailto:r.raiswell@earth.leeds.ac.uk), fax 0113343 5259

**Abstract**

DSDP/ODP porewater profiles in organic carbon-bearing (< 5% org. C) sediments commonly show decreases in  $\text{Ca}^{2+}$  concentrations and increases in alkalinity over depths where sulphate is being removed by microbial reduction. These  $\text{Ca}^{2+}$  depletion profiles represent the combined effect of diffusion, advection and reaction (addition by ion exchange and removal by precipitation mainly as  $\text{CaCO}_3$  and/or dolomite). A diagenetic model has been used to estimate the rate constant (k) for  $\text{Ca}^{2+}$  removal by precipitation during sulphate depletion over depths of 15-150 m, assuming first order kinetics. The rate constants for  $\text{Ca}^{2+}$  removal range from  $10^{-14}$  to  $10^{-11}\text{s}^{-1}$  in 19 DSDP/ODP sediments, which span a range of bottom water temperatures (0-10°C), lithologies (calcareous to clastic) and sedimentation rates (0.001-0.4  $\text{cm yr}^{-1}$ ). Values of k correlate with sedimentation rate ( $\omega$ ) such that  $\log k = 1.16 \log \omega - 10.3$ , indicating that faster rates of  $\text{Ca}^{2+}$  removal occur at higher sedimentation rates where there are also higher degrees of saturation with respect to  $\text{CaCO}_3$  and dolomite. Depth-integrated masses of  $\text{Ca}^{2+}$  removed (<100  $\mu\text{mol cm}^{-2}$ ) during sulphate depletion over these depth ranges are equivalent to a dispersed phase of approximately 1.5 wt.%  $\text{CaCO}_3$  or 3 wt.% dolomite in a compacted sediment. The complete occlusion of sediment porosity observed in concretions with isotopic signatures suggesting carbonate sourced from sulphate reduction therefore requires more time (a depositional hiatus),

more rapid sulphate reduction (possibly by anaerobic methane oxidation) and/or the continued transport of isotopically light carbonate to the concretion site after sulphate reduction has ceased.

*Keywords:* Carbonate cementation, Concretions, Sulphate reduction.

## 1. Introduction

Carbonate concretions occurring in ancient marine sediments from continental shelf, slope and deep basinal environments commonly have light carbon isotope compositions, which are invariably interpreted to indicate that the carbonate has been derived from the microbial mineralisation of organic matter (Mozley and Burns, 1993). Various lines of evidence (the deformation of host sediment laminae around concretions, the presence of uncrushed fossil material and septarian fissures) indicate that cementation must have been able to resist the effects of compaction, and thus must have been at least initiated at shallow burial depths (Raiswell and Fisher, 2000). These three lines of evidence are consistent with the porewater chemistry of modern sediments (Canfield and Raiswell, 1991), which are generally over-saturated with respect to  $\text{CaCO}_3$  and dolomitic phases at shallow depths where organic carbon is undergoing microbial decay.

Organic carbon undergoes microbial decay to dissolved carbonate species ( $\Sigma\text{CO}_2$ ) via a sequence of processes that utilise dissolved oxygen, nitrate, iron and manganese oxides and sulphate as electron acceptors (e.g. Froelich et al., 1979; Thamdrup and Canfield, 1996). These decay processes are usually limited by the decline in availability (or reactivity) of electron acceptors with increasing depth, after which microbial activity produces methane mainly by  $\text{CO}_2$  reduction. Methane may diffuse upwards to become an important source of organic matter for sulphate reduction (Devol, 1983; Iverson and Jorgensen, 1985; Boetius et al., 2000) by anaerobic methane oxidation (AMO).

Most organic carbon decay occurs by iron reduction and sulphate reduction (Canfield, et al., 1993; Thamdrup, 2000) and the  $\Sigma\text{CO}_2$  reflects the isotopic composition of the organic matter and is thus isotopically light. Consistent with this, Mozley and Burns (1993) observed that the  $\delta^{13}\text{C}$  compositions (all values with respect to PDB) of calcite ( $-22$  to  $+3$  ‰) and dolomite ( $-20$  ‰ to  $+25$  ‰) concretions typically have minimum values as expected for carbonate derived from organic matter ( $-22$  to  $-28$  ‰). The range to significantly heavier isotopic values may arise from the addition of carbonate derived from overlying seawater, skeletal material or from methanogenesis by  $\text{CO}_2$  reduction (which produces isotopically light methane and leaves residual  $\Sigma\text{CO}_2$  that is isotopically heavy; Claypool and Kaplan, 1974). Mozley and Burns (1993) proposed that calcite concretions formed in sediments in which the rates of sulphate reduction were relatively low (poorly reactive organic matter), and which thus maintained active sulphate reduction to relatively large burial depths. Conversely, dolomite concretions were favoured when

more rapid sulphate reduction (more reactive organic matter) produces thinner zones of sulphate reduction. In the latter circumstances sufficient labile organic matter may exist to allow more extensive methanogenesis, which can be initiated nearer the sediment surface and maintained over greater depths. Such conditions were argued to increase the likelihood that concretionary growth would produce very positive  $\delta^{13}\text{C}$  values.

Mozley and Burns (1993) clearly envisaged that concretionary growth is initiated in the zones of sulphate reduction. Stoichiometric closed system models of sulphate reduction show that porewaters become oversaturated with respect to carbonates, and thus provide support for this conclusion. Ben Yaakov (1973) showed that the effects of sulphate reduction



depend on whether the  $\text{H}_2\text{S}$  accumulates in the porewaters or is removed by precipitation as iron sulphide. Both cases produced porewaters that were oversaturated with  $\text{CaCO}_3$ , but the precipitation of sulphide increased pH and produced greater oversaturation. More detailed studies considering the combined effects of oxic respiration, denitrification and sulphate reduction in both closed (Canfield and Raiswell, 1991) and open system models (Boudreau and Canfield, 1993) confirm that significant oversaturation with respect to  $\text{CaCO}_3$  arises whether sulphide accumulates or precipitates (except for small increments of sulphate removal, see below).

Several decades of porewater studies in modern sediments have however failed to show carbonate cementation occurring during sulphate reduction (as distinct from AMO; see below) on a scale sufficient to form concretions analogous to those found in ancient sediments. Porewaters, although often over-saturated with respect to  $\text{CaCO}_3$ , appear to be kinetically inhibited from precipitation by the presence of phosphate, magnesium, sulphate and organic matter (Walter, 1986; Morse and Mackenzie, 1990). The precipitation of dolomite also appears to be kinetically inhibited by the presence of sulphate (for an alternative view see Morrow and Ricketts, 1986), but is progressively favoured by high Mg/Ca ratios and high concentrations of alkalinity (Baker and Kastner, 1985; Compton, 1988).

Collectively these studies suggest the production of no more than a diffuse volume of concretionary cement whilst sulphate is being depleted by microbial reduction, but that this cement provides a porous framework which is sufficient to resist compaction. Thus the rates of cement precipitation are likely to be too slow to produce visual or measurable evidence of cementation in modern sediments. However many DSDP/ODP modern sediments (Fig. 1) do contain porewater profiles showing  $\text{Ca}^{2+}$  depletion over considerable (decimetre-scale) burial depths, indicating rates

of  $\text{Ca}^{2+}$  -removal (by the sum of different precipitation processes, see below) are able to equal or exceed rates of transport supply from overlying seawater by diffusion and advection.

Depletion of  $\text{Ca}^{2+}$  in these DSDP/ODP sediments mainly represents the combined effect of transport by diffusion and advection, plus removal by precipitation both as authigenic carbonate ( $\text{CaCO}_3$ , dolomite) and phosphate minerals. Modelling precipitation rates based on  $\text{Ca}^{2+}$  depletion is simpler than modelling changes in  $\Sigma\text{CO}_2$  which would also require estimates of the rates of  $\Sigma\text{CO}_2$  addition by microbial decay. Middelburg (1990) has derived two diffusion-advection-reaction diagenetic models based on Berner (1980) to describe  $\text{Ca}^{2+}$  depletion profiles in the sediments at Kau Bay, Indonesia. The diagenetic equations derived for these profiles allow the rate constant for  $\text{Ca}^{2+}$  removal to be estimated. It is the purpose of this paper to use one of these diagenetic models to estimate the rate constants for (and rates of)  $\text{Ca}^{2+}$  removal during sulphate depletion from a range of DSDP/ODP sediments with different lithological and sedimentological characteristics. These rates of  $\text{Ca}^{2+}$  removal are then used to provide order of magnitude estimates of the extent of carbonate cementation that can occur when sulphate reduction takes place over relatively large burial depths. Finally, the implications for concretion growth are explored. In particular, the reasons are discussed as to why concretions directly analogous to those within the ancient geological record are not found in modern sediments.

## 2. Approach

Many DSDP/ODP sediments have near-surface porewater data showing continued losses of  $\text{Ca}^{2+}$  with depth accompanied by increases in alkalinity (and other dissolved products of microbial decay) and decreases in sulphate concentrations. Figure 1 shows two such profiles from sites 533 (Blake Outer Ridge) and 931 (Amazon Fan), which have comparable lithologies and porosities but different sedimentation rates (see Table 1). We have selected 19 DSDP/ODP sites (Table 1) that meet the following criteria;

- (1) All are fine-grained sediments containing low to moderate concentrations of organic carbon (< 5 wt. %) along with variable proportions of clastic and biogenic (calcareous, siliceous) components.
- (2) Sulphate decreases slowly with depth (over 15-150m) and concentrations are greater than approximately 1 mM over the studied depths, except at sites 798, 819, 821, 911, 931, 939B, 939C, 942 and 944 (where sulphate concentrations fall to 0.1 mM for more than half the depth

studied). Methane is present at low concentrations over these depths but there is no evidence of AMO.

- (3) The depth profiles show a ‘concave down’ decrease in  $\text{Ca}^{2+}$ , and an increase in alkalinity. These ‘concave-down’  $\text{Ca}^{2+}$  depletion profiles indicate the progressive removal of  $\text{Ca}^{2+}$  through the depths over which sulphate is being reduced and result from the net effects of  $\text{Ca}^{2+}$  addition mainly by diffusion from overlying seawater and by advection, and  $\text{Ca}^{2+}$  removal by precipitation. The site descriptions either infer carbonate precipitation from these profiles or, occasionally, there is visual evidence of carbonate precipitation.
- (4) Porewater values of pH,  $\text{Ca}^{2+}$  and alkalinity are available that allow calculation of the Saturation Index (SI) as  $\text{Log}(\text{Ion Activity Product}/K_{\text{sp}})$  with respect to  $\text{CaCO}_3$  and  $\text{CaMg}(\text{CO}_3)_2$ . The SI data are useful only for comparative purposes (Gieskes, 1974) as pressure release during core retrieval causes  $\text{CO}_2$  degassing and hence produces a pH increase that may induce carbonate precipitation (Morse, 1983) and hence alter the in situ SI values.
- (5) No quantitatively significant breaks in sedimentation have been recorded over that part of the section under consideration, and the average sedimentation rate is known.
- (6) The bottom water temperature, and the porosity of the sediments over the chosen interval, are both known.

Criteria (1) and (2) together ensure that the sediments are undergoing sulphate reduction, that rates of sulphate depletion (and therefore reduction) are slow, and that AMO does not exert a significant influence over the studied depths. Criteria (3) provides an indication that carbonate precipitation is occurring, which criteria (4) may support by calculation of the SI values. Criteria (5) and (6) provide the necessary data to allow calculation of  $\text{Ca}^{2+}$  removal rates from a diagenetic equation that considers supply by diffusion, advection and ion exchange and removal by precipitation.

The general diagenetic equation for a dissolved component in porewater can be written (Berner, 1980; Boudreau, 1996) as;

$$D_s \frac{d^2C}{dx^2} - \omega (1 + K) \frac{dC}{dx} - k (C - C_{\text{eq}}) = 0 \quad (1)$$

where  $D_s$  ( $\text{cm}^2 \text{s}^{-1}$ ) is the diffusion coefficient corrected for tortuosity effects (approximated from porosity data, see below),  $C$  is the concentration of  $\text{Ca}^{2+}$  ( $\text{mmol cm}^{-3}$ ),  $C_{\text{eq}}$  is the steady state concentration of  $\text{Ca}^{2+}$  ( $\text{mmol cm}^{-3}$ ),  $\omega$  is the sedimentation rate ( $\text{cm s}^{-1}$ ),  $K$  is the linear adsorption constant and  $k$  ( $\text{s}^{-1}$ ) is the rate constant for  $\text{Ca}^{2+}$  removal. The model assumes that steady state diagenesis occurs and that the  $\text{Ca}^{2+}$  profiles reflect the effects of diffusion, advection and reaction.

The reactions that affect  $\text{Ca}^{2+}$  are assumed to be additions by rapid equilibrium ion exchange plus removal by precipitation of authigenic minerals (see below). It is also assumed that no  $\text{Ca}^{2+}$  is supplied by the dissolution of carbonates in the surrounding sediments (see below).

Our DSDP/ODP sediments typically contain hundreds of  $\mu\text{M}$  (and up to a maximum of 6 mM) ammonium generated through the decomposition of nitrogen-bearing organic matter (Berner, 1980). Ammonium has a strong affinity for ion exchange sites and has been observed to readily displace  $\text{Ca}^{2+}$ ,  $\text{Mg}^{2+}$  and  $\text{K}^{+}$  from clays in DSDP/ODP sediments (e.g. Gieskes, 1983). The effects of ion exchange are incorporated into the diagenetic equation by a simple linear isotherm, using a value of 1.6 for the dimensionless adsorption constant (Berner, 1980). This approach only provides an order of magnitude estimate of the effects of ion exchange. Rate constants for  $\text{Ca}^{2+}$  removal derived for our DSDP/ODP sites in the presence of ion exchange effects are only about 20-40% lower than in their absence (which is comparable to the uncertainty in our estimates, see below).

The diagenetic model assumes linear first order kinetics for  $\text{Ca}^{2+}$  removal although experimental studies of calcite precipitation in seawater (Mucci and Morse, 1983; Burton and Walter, 1987; Mucci et al., 1989; Zhong and Morse, 1993) show that the precipitation kinetics follow a rate law of the form;

$$\text{Rate} = k (\Omega - 1)^n \quad (2)$$

where  $k$  is the rate constant,  $n$  is the reaction order and  $\Omega$  is the Saturation Index (defined as Ion Activity Product/ $K_{sp}$ ). Burton and Walter (1987) have shown that values of  $n$  for aragonite and calcite can vary from 0.4 (at 5°C) to approx 2.4 (at 37°C). There are rather fewer studies of dolomite but a similar rate law (with  $n = 2.2$  at 25°C) has been found by Arvidson and Mackenzie (1999). Morse and Arvidson (2002) have demonstrated the inadequacy of first order kinetic models that ignore the complexities of near-equilibrium carbonate mineral reaction kinetics. The models used here are not intended to challenge this view, but the precipitation kinetics of the DSDP/ODP sediments studied here are likely to be much more complex (and to have different reaction orders) than the experimental systems which utilise relatively simple compositions at laboratory temperatures (compared to the bottom temperatures in Table 1). The kinetic behaviour of the DSDP/ODP porewaters may also be modified by a variety of factors. Firstly,  $\text{Ca}^{2+}$  removal into the DSDP/ODP sediments may occur by precipitation into a mixture of poorly-characterised, impure phases such as aragonite, calcite, high Mg calcite, dolomite and carbonate fluorapatite (CFA). Secondly,  $\text{Ca}^{2+}$  removal is strongly influenced by the presence of inhibitors (see earlier). Berner and Morse (1974) and Mucci (1986) have shown that phosphate is an extremely strong

inhibitor of carbonate precipitation kinetics at  $\mu\text{M}$  levels (as are found in these DSDP/ODP porewaters), as also is organic matter (Berner, 1975). The precipitation kinetics of dolomite and  $\text{CaCO}_3$  are not sufficiently well-known under such diagenetic conditions to justify using complex kinetic expressions, and thus we argue that a first order model is able to provide an order of magnitude approximation to the kinetics of  $\text{Ca}^{2+}$  removal in our the DSDP/ODP sediments over the small variations of SI in our cores (Table 2). Luff and Wallmann (2003) have also used a first order model for the diagenetic precipitation of carbonates formed by AMO, for similar reasons.

The upper boundary conditions for equation (1) are specified by setting the concentration of  $\text{Ca}^{2+}$  as equal to the bottom water concentration ( $C_o$ );

$$x = 0 \text{ and } C = C_o$$

and the lower boundary condition is given by

$$x \rightarrow \infty \text{ and } C \rightarrow C_{\text{eq}}$$

With these boundary conditions Berner (1980) and Boudreau (1996) state that the solution of equation (1) is;

$$C - C_{\text{eq}} = (C_o - C_{\text{eq}}) \exp \left[ \frac{\omega (1 + K) - \{\omega^2 (1 + K)^2 + 4kD_s\}^{0.5}}{2D_s} \right] x \quad (3)$$

The infinite dilution diffusion coefficient ( $D^0$ ) for  $\text{Ca}^{2+}$  is derived from Boudreau (1996) as  $D^0$  ( $\text{cm}^2 \text{ s}^{-1}$ ) =  $(3.6 + 0.179 T^\circ\text{C}) 10^{-6}$ . The corrections for tortuosity are derived from Ullman and Aller (1982) who give  $D_s = D^0/\phi F$ , where  $\phi$  is the porosity and the Formation Factor  $F$  is approximated as  $1/\phi^m$  and  $m = 2.5$  to  $3.0$  for muddy sediments. Simplifying thus approximately produces;

$$D_s = D^0\phi^{1.7} \quad (4)$$

### 3. Results

Table 2 summarises the chemical characteristics of each site. No bottom water data were available at sites 819A and 944D and an average seawater  $\text{Ca}^{2+}$  concentration (10.5 mM) was therefore used. Equation (3) was solved by fitting an exponential curve to the depth profiles of  $\text{Ca}^{2+}$ . A trial and error approach was adopted to identify the maximum depth from the surface over which the best fit was achieved. Most sites had best fit correlation coefficients that were significant at the 0.1% level or less, but five sites had correlation coefficients with about 1% significance

levels (565, 722A, 908A, 911A and 939B). These were retained to improve the range in physical and chemical characteristics of the sample suite. The exponential term in equation (3) was then set to equal the exponential term in the best fit equation and solved for  $k$ . Values of  $k$  are listed in Table 2.

Uncertainties have been estimated on the  $\text{Ca}^{2+}$  concentrations,  $\phi$ ,  $D_s$  and  $\omega$  as follows. Gieskes (1974) estimates the precision on the  $\text{Ca}^{2+}$  analyses as 0.2%. We assume negligible uncertainties on the depth measurements and no porosity changes with depth. Our sites show trends of decreasing porosity with depth, but these are erratic and the depth ranges used are relatively small (mostly < 50m). The assumption of no porosity changes allows the use of constant average values for  $K$  and  $D_s$ , which introduce negligible uncertainties compared to those resulting from other assumptions (Berner, 1980). The coefficient of variation of the mean porosity is generally around 10% and this figure has been utilised as a precision on  $\phi$  and carried through equation (3) to produce a mean uncertainty on  $D_s$  of approximately 17%. Berner (1980) gives two values for  $K$  (1.4 and 1.8) and we have therefore used  $1.6 \pm 0.1$  to estimate the uncertainty from  $K$  in equation (2). Inspection of the DSDP/ODP literature gives little information on uncertainties in  $\omega$  but different estimates of  $\omega$  are available for a few sites and these suggest an uncertainty of approximately  $\pm 20\%$  may be reasonable. The calculated values (and their uncertainties) for the rate constant ( $k$ ) are given in Table 2.

The Saturation Indices (SI) for calcite and dolomite have been derived using SOLMINEQ (Kharaka and Barnes, 1973) for the intervals over which  $k$  has been estimated. The SI values have been derived at the observed bottom water temperatures, using a laboratory measurement temperature of 25°C. In most cases there is sufficient major element data to allow a reasonable estimate of SI which takes full account of ionic strength and ion pairing effects. However in a few cases Na and Cl have not been measured and average values for seawater have then been used. Charge balance errors never exceed 5% and are frequently lower. The range of SI values over each depth interval are also given in Table 2 and considerable down core variation can clearly occur. The influence of sampling artefacts (see above) only allow the SI data to be used qualitatively to compare site behaviour.

## **4. Discussion**

### *4.1 Porewater profiles and authigenic mineralogy*

The sites used in this study cover a range of lithologies, porosities, bottom water temperatures and sedimentation rates (Table 1). Some of these sites show visual evidence of carbonate precipitation, usually as calcite and/or dolomite, occasionally accompanied by an apatitic phase. It is unfortunately impossible to apportion  $\text{Ca}^{2+}$  removal rates between these three minerals. Our sites were chosen to contain relatively thick zones of sulphate reduction (e.g. compare with Berner, 1980) which has been argued to favour calcite precipitation (see above and Mozley and Burns, 1993). However the  $\text{Ca}^{2+}$  depletion in these DSDP/ODP sediments is commonly accompanied by magnesium concentrations that decrease with depth (but rarely fall below 30 mM), consistent with dolomite precipitation. Unfortunately Mg profiles are also affected by several other processes, including removal into silicates to replace Fe used for pyrite formation (e.g. Drever, 1974), and by ion exchange both replacing  $\text{Ca}^{2+}$  (Russell, 1970) and being replaced by  $\text{NH}_4^+$  produced by organic matter decay (see above). It is difficult to estimate the relative contributions of these different processes, and thus Mg depletions cannot be used to estimate rates of dolomite formation. A further complication is that dolomite compositions can vary from near stoichiometric (Middelburg et al., 1990) to a calcium-rich protodolomite (Compton, 1988).

Authigenic dolomite does however form in organic carbon-bearing sediments such as those discussed here (Baker and Burns, 1985; Compton, 1988; Middelburg et al., 1990) where the kinetic barriers to precipitation are diminished. The formation of these 'organogenic' dolomites is assisted by the process of sulphate reduction, which adds alkalinity (thus enhancing the degree of dolomite oversaturation; Hardie, 1987), and removes sulphate (which is believed to inhibit dolomite precipitation; Baker and Kastner, 1985; Compton, 1988). It is argued that even minor concentrations of sulphate strongly inhibit dolomite precipitation (Baker and Kastner, 1985; Compton, 1988). Sulphate is not completely depleted from most of our DSDP/ODP cores (see criteria 2), but at least some of our sediments contain authigenic dolomite.

The profiles of  $\text{Ca}^{2+}$  depletion are also likely to be influenced by the formation of CFA. The phosphorus released from organic matter mineralisation and the dissolution of Fe oxyhydroxides produces porewaters that are oversaturated with respect to CFA, although precipitation is slow (Van Cappellen and Berner, 1991; Ruttensburg and Berner, 1993). Concentrations of porewater phosphate in modern sediments (and in our DSDP/ODP profiles) never reach beyond mM levels and, consistent with this, estimated rates of P accumulation are extremely slow (for example ~0.003 wt % at FOAM; Ruttensburg and Berner, 1993). These observations suggest that CFA precipitation is unlikely to produce a significant influence on our

Ca<sup>2+</sup> depletion profiles, except possibly at the slowest sedimentation rates. However some sediments show visual accumulation of apatitic phases, possibly representing re-working of authigenic phases (Ruttenburg and Berner, 1993). Phosphate concentrations are also controlled by a variety of processes including additions by organic matter decay and exchange on to clays and, as before, the existence of these competing reactions prevents the porewater chemistry from providing any simple constraint on the rates of CFA precipitation. Clearly our Ca<sup>2+</sup> removal rates cannot be confidently attributed to carbonate precipitation alone, and instead represent only the maximum possible rates of carbonate precipitation (by CaCO<sub>3</sub> or dolomite), assuming no Ca<sup>2+</sup> is supplied by carbonate dissolution in the surrounding sediments (see below).

#### *4.2 Rate constants: magnitude and dependence on $\omega$ and SI .*

Rate constants for Ca<sup>2+</sup> removal during sulphate reduction vary from  $1.2 \times 10^{-14}$  to  $3 \times 10^{-11}$  s<sup>-1</sup> for the DSDP/ODP sediments (Table 2) but cannot be compared with published values, which are usually derived experimentally from rate laws such as equation (2) in which k has units of mass area<sup>-1</sup> time<sup>-1</sup>. Values in these units have been reported for calcite precipitation from seawater by Mucci and Morse (1983), Mucci (1986), Burton and Walter (1987) and Zhong and Muci (1993), but comparisons would require sensible estimates of the surface area of the precipitating phases in these DSDP/ODP sediments which are impossible.

However the rate constants for Ca<sup>2+</sup> removal in the DSDP/ODP sediments can be compared to the Kau Bay data of Middelburg (1990), who estimated rate constants for Ca<sup>2+</sup> removal for three cores which ranged from  $1.6 \times 10^{-9}$  (core K3) to  $1.6 \times 10^{-10}$  s<sup>-1</sup> (cores K4 and K11). These estimates used a rather more complex diagenetic model than the one used here and our model using the Middelburg (1990) data produces  $7 \times 10^{-10}$  s<sup>-1</sup> for K3 and  $1 \times 10^{-10}$  s<sup>-1</sup> for K4. Both these rate constants are within a factor of 2 of those estimated by Middelburg (1990) and are also comparable to the k values found in the DSDP/ODP sediments, since there is a significant temperature difference between the Kau Bay bottom waters (30°C) and the DSDP/ODP bottom waters (0-10°C; see Table 1). The comparable magnitudes of the rate constants for Ca<sup>2+</sup> removal in the DSDP/ODP sediments and the Kau Bay cores, together with the well-documented occurrence of dolomite in the Kau Bay sediments (Middelburg et al., 1990) are consistent with dolomite precipitation as the principal mechanism of Ca<sup>2+</sup> removal in the DSDP/ODP sediments, as has been suggested elsewhere (Compton, 1988).

The values for the rate constants, saturation indices and sedimentation rates are all closely related. Our DSDP/ODP data give a good correlation between  $\log k$  and  $\log \omega$  (Fig. 2) such that;

$$\log k = 1.16 \log \omega - 10.3$$

and the correlation coefficient  $r = 0.85$  is significant at the  $<0.1\%$  level. This suggests that faster rates of  $\text{Ca}^{2+}$  removal occur at the highest sedimentation rates, where the most labile organic matter is buried and the highest rates of sulphate reduction occur (see Toth and Lerman, 1977; Boudreau, 1996). Consistent with this, Fig. 3 shows that the maximum SI values of calcite and dolomite (see Table 2) both follow a fairly smooth curvilinear trend of increasing SI with increasing sedimentation rate.

The data in Fig. 3 tend to level off at high SI values because increases in  $k$  (the rate constant for  $\text{Ca}^{2+}$  removal) tend to produce increasing rates of precipitation, and thus decrease calcium and carbonate ion activities in the porewaters (hence decreasing  $\text{SI}_{\text{cal}}$  and  $\text{SI}_{\text{dol}}$ ). However increases in  $k$  are also associated with faster rates of alkalinity generation (see above), which tend to produce increases in the carbonate ion activity (which may be modified by pH changes). Ultimately these two opposing effects on the SI values balance out when rates of calcium removal by precipitation are matched by the combined effects of increasing carbonate ion activity through sulphate reduction and decreasing carbonate ion activity by precipitation. The existence of these opposing effects means that higher rate constants will not necessarily produce commensurate increases in  $\text{SI}_{\text{cal}}$  and  $\text{SI}_{\text{dol}}$ .

#### 4.3 Masses of carbonate precipitated during sulphate reduction.

The diagenetic model assumes that the rate of  $\text{Ca}^{2+}$  removal ( $R$ ) by precipitation is given by the first order relationship:

$$R = \frac{dC}{dt} = -k(C - C_{\text{eq}}). \quad (5)$$

Hence the integrated rate of  $\text{Ca}^{2+}$  removal can be calculated as:

$$\Sigma R = \frac{1}{\omega} \int R dx.$$

So

$$\Sigma R = \frac{-k}{\omega} \int (C - C_{\text{eq}}) dx \quad (6)$$

and this equation can now be integrated with respect to  $x$  after substituting for  $(C - C_{eq})$  from equation (3), and expressing concentrations in  $\text{mmol cm}^{-3}$  of sediment plus pore fluid. Thus;

$$\Sigma R = -\frac{\phi k}{\omega} (C_o - C_{eq}) \int \exp. (Bx) dx \quad (7)$$

$$\text{where } B = \frac{\omega (1 + K) - \{\omega^2 (1 + K)^2 + 4kD_s\}^{0.5}}{2D_s}.$$

Integrating equation (7) produces;

$$\Sigma R = \left[ -\frac{\phi k}{\omega B} (C_o - C_{eq}) \exp. (Bx) \right]_{x=0}^{x=\infty}$$

However when integrating from 0 to  $\infty$ , the term  $B$  is small ( $10^{-3}$  to  $10^{-4}$ ; see Table 2) and negative, so that at large depths ( $> 10^4$  cm) the exponential term tends to zero. Similarly at  $x = 0$ ,  $\exp. (Bx) = 1$  and the maximum value of  $\Sigma R$  ( $\text{mol cm}^{-2}$ ) integrated over the studied depths is given by;

$$\Sigma R = -\frac{\phi k}{\omega B} (C_o - C_{eq}). \quad (8)$$

The depth-integrated masses of  $\text{Ca}^{2+}$  calculated from equation (8) are reported in Table 2 using the appropriate value of  $C_o$  for each site (within 10% of mean seawater  $\text{Ca}^{2+}$  at  $0.0105 \text{ mmol cm}^{-3}$ ) and assuming  $C_{eq} = 0$ . The term  $\Sigma R$  represents the maximum mass of  $\text{Ca}^{2+}$  that can be precipitated during sulphate reduction in these DSDP/ODP cores. The maximum masses show only small variations and are typically  $< 100 \mu\text{mol Ca}^{2+} \text{ cm}^{-2}$ . The removal of  $\text{Ca}^{2+}$  as calcite produces a smaller volume of calcite cement than dolomite (1:1.58) and the maximum mass of  $\text{Ca}^{2+}$  removed would only represent a dispersed phase of about 1.5 wt.% of calcite or 3 wt.% dolomite in these sediments (after complete removal of remaining porosity by compaction). Consistent with observations of modern sediments, the models predict that only small concentrations of carbonate cement can precipitate during sulphate reduction, even over comparatively large burial depths.

Complete occlusion of host sediment porosity clearly requires substantially larger masses of carbonate cement. Consider a  $1 \text{ cm}^3$  of sediment that has  $0.7 \text{ cm}^3$  of pore space available to achieve complete cementation ( $\phi = 0.7$ ). For  $\text{CaCO}_3$  (density of  $2.7 \text{ g cm}^{-3}$ ) and  $\text{CaMg}(\text{CO}_3)_2$  (density  $2.9 \text{ g cm}^{-3}$ ) complete cementation requires approximately 0.019 mol of  $\text{CaCO}_3$  or 0.01 mol of  $\text{CaMg}(\text{CO}_3)_2$ , which is roughly 500-1000x larger than the amounts estimated in Table 2.

Viewed in this context, the models of  $\text{Ca}^{2+}$  removal used here are consistent with Raiswell and Fisher (2000), who proposed that early cementation during sulphate reduction could only be sufficient to produce a framework which could resist compaction. However below we examine other factors that may produce increased cementation above the steady state model values derived here.

#### 4.3.1 *More rapid rates of sulphate reduction.*

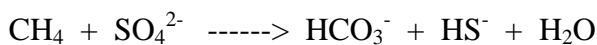
The DSDP/ODP sediments studied here are possibly atypical in that rates of sulphate reduction (and hence rates of  $\text{Ca}^{2+}$  removal) may be slower than in ancient concretion-bearing sediments. In general, the rate constants for organic matter decay by sulphate reduction ( $k_{\text{ORG}}$ ) vary with sedimentation rate. For example, Tromp et al. (1995) have up-dated the Toth and Lerman (1977) data to show that;

$$\log k_{\text{ORG}} = 1.94 \log \omega + 0.057.$$

Thus more rapid rates of cementation may be possible in sediments with greater concentrations of more labile organic matter which produce faster rates of sulphate reduction. However the integrated rates of  $\text{Ca}^{2+}$  removal vary by much less than one order of magnitude (Table 2) despite large variations in sedimentation rate (nearly 3 orders of magnitude; see Table 1). This is because the variations in  $k/\omega$  and  $B$  occur in opposite directions over the studied depth ranges. Equation (8) shows the relationship between the depth- integrated masses of  $\text{Ca}^{2+}$  removed ( $\Sigma R$ ) and  $k$ ,  $\omega$ ,  $\phi$  and  $B$ , and recall that  $C_0$  and  $\phi$  are assumed constant and that  $B$  is small and negative (see Table 2). Thus  $\Sigma R$  is large when  $(-k/\omega B)$  is large and positive. However  $\log k$  covaries with  $\log \omega$  (Fig. 2), such that  $k/\omega$  increases only slowly for  $\omega < 1\text{cm/yr}$  (over the studied depth ranges) and produces only small increases in  $\Sigma R$ . Conversely  $B$  (the negative exponent) also increases slowly (but erratically) with  $\omega$  (see Tables 1 and 2), which causes  $\Sigma R$  to decrease. Hence the effects of  $k/\omega$  and  $B$  to a significant degree cancel each other out for  $\omega < 1\text{cm/yr}$ . The estimates of  $\Sigma R$  in Table 2 are generally higher at faster sedimentation rates but some exceptions exist where porosities are relatively low, or where sites show deviations from the overall trends. Larger increases in  $\Sigma R$  may occur where  $\omega > 1\text{cm/yr}$  (since  $k/\omega$  then increases rapidly with  $\omega$ ), but we have no data on the behaviour of  $B$  to justify extrapolation to these sedimentation rates. However we note that concretionary cementation is commonly associated with slowly deposited, organic C-rich sediments (eg Fisher and Wignall, 2001) rather than with rapidly-deposited sediments.

The DSDP/ODP sediments studied here are all deposited under oxygenated bottom waters whereas sediments beneath anoxic bottom waters generally show faster rates of sulphate reduction (and thus alkalinity generation), and possibly therefore also faster increases in  $\Sigma R$  with  $\omega$ . However it is doubtful whether bottom water oxygenation could exert a critical control on concretionary growth for two reasons. Firstly, carbonate concretions are commonly found in depositional environments ranging from fully oxygenated and bioturbated (e.g. Savrda and Bottjer, 1988) to oxygen-deficient/euxinic (e.g. Raiswell, 1976). Secondly, rate constants for the semi-euxinic Kau Bay sediments follow the same general trend with respect to  $\log \omega$  as do the DSDP/ODP sediments (see above). Additional data for the rate constants of  $Ca^{2+}$  removal from sediments deposited under anoxic bottom waters are needed to ascertain whether higher rates of  $Ca^{2+}$  removal can occur under euxinic conditions, but the limited data here do not suggest that bottom water oxygenation levels exert a significant influence.

Rates of sulphate reduction at depth (after most labile organic matter has been mineralized) can however be stimulated by AMO (Devol and Ahmed, 1981; Devol, 1983; Iverson and Jorgensen, 1985) which has been identified as a likely source of concretionary carbonate (Raiswell, 1987; 1988a). In this context it is noteworthy that carbonate cementation has been well-documented in ODP cores from the Blake Outer Ridge at Sites 994, 995, 996 and 997 (Naehr et al., 2000; Rodriguez et al., 2000). At sites 994, 995 and 997, Rodriguez et al. (2000) found that sulphate reduction occurred in an upper zone (0 to 20 m) through which the porewater gradients indicate either active calcite dissolution plus reprecipitation or simple diffusion between seawater and a lower zone of AMO. Calcite (10-45 wt.%) and dolomite (1-8 wt.%) in this zone have isotopic compositions that indicate a mainly biogenic origin but small concentrations of authigenic carbonate may occur at below detection levels. The 20 m depth defines a biogeochemical interface where methane, building up in the sediments below, diffuses up to be consumed by AMO



along with sulphate diffusing downwards. Over the 20-100 m depth interval authigenic dolomite predominates over calcite and occurs as discrete microcrystalline nodules (< 6 cm diameter) which contain concentrations of 2-40 wt. % dolomite. The  $\delta^{13}C$  values of calcite are slightly negative (minimum of  $-7 \text{ ‰}$ ) as also is dolomite ( $-3$  to  $-14 \text{ ‰}$ ). At site 996, Naehr et al. (2000) also found extensive cementation but the predominant mineralogy was aragonite (23-63 wt. %) with  $\delta^{13}C$  values of  $-30$  to  $-48 \text{ ‰}$ . Luff and Wallmann (2003) have modelled the rates of carbonate precipitation by AMO at the Cascadia Margin. Aragonite and calcite are the main authigenic

phases and precipitate at a rate of  $120 \mu\text{mol cm}^{-2} \text{yr}^{-1}$ , sufficient to form a 1 m thick layer in approximately 20000 years.

These studies are consistent with the present work in demonstrating that sulphate reduction (as distinct from AMO) can only produce limited amounts of carbonate cement but AMO can clearly be an important source of carbonate cement. There are however significant difficulties in explaining the absence of very light  $\delta^{13}\text{C}$  values ( $<30 \text{‰}$ ) in most concretions (Mozley and Burns, 1993), although such values are common in carbonates formed by AMO. A consideration of the isotopic signals that can result from AMO is beyond the scope of the present work but has been dealt with by Claypool and Threlkeld (1983) and Raiswell (1987).

#### 4.3.2 Additional $\text{Ca}^{2+}$ sources during sulphate reduction

The diagenetic model used here has assumed that all  $\text{Ca}^{2+}$  is supplied by diffusion from seawater. In this section we explore whether internal sources of  $\text{Ca}^{2+}$  could contribute to the formation of additional cement during sulphate reduction. The DSDP/ODP sediments are all over-saturated with respect to both calcite and dolomite (see Table 2), which would seem to preclude the supply of additional  $\text{Ca}^{2+}$  from the dissolution of biogenic calcareous debris during sulphate reduction. However diagenetic models (Canfield and Raiswell, 1991; Boudreau and Canfield, 1993) predict that calcite and aragonite can become under-saturated if sulphide accumulates in the porewaters during the early stages of sulphate reduction (removal of up to 5-7 mM  $\text{SO}_4^{2-}$ ). Such under-saturation must be confined to micro-environments (since the bulk SI values in the DSDP/ODP sediments indicate over-saturation), which would suggest that carbonate dissolution could only have a limited impact during sulphate reduction (the dissolution of biogenic carbonate may however be a significant source during subsequent burial).

Biogenic carbonate is not the only source of  $\text{Ca}^{2+}$ . Dissolution of fish debris is thought to be an important source of solutes for apatite precipitation (e.g. van Cappellen and Berner, 1988) and could also be a potential source of  $\text{Ca}^{2+}$  for carbonate cementation. It is worth noting that TEM studies have revealed that amorphous Fe-oxides can contain up to 6%  $\text{Ca}^{2+}$  (Buffle et al., 1989). Iron oxides of this type would be expected to undergo reduction following sedimentation and therefore could potentially provide an additional source of  $\text{Ca}^{2+}$  for concretion growth.

#### 4.3.3 Non steady state diagenetic effects

The estimates of  $\Sigma\text{R}$ , and their variations with sedimentation rate, are not apparently adequate to provide more than low concentrations of cement when sulphate reduction occurs over considerable burial depths. Higher concentrations may be possible in non-steady state depositional

environments, where a pause in deposition allows the continued supply of sulphate and calcium from seawater, enabling precipitation to be maintained over a shallow depth interval (where SI values are appropriately high) for sufficient lengths of time to produce greater masses of cement. The effects of a pause in deposition were also suggested by Middelburg et al. (1990) to account for the dolomitic concretionary layers observed in the Kau Bay sediments. The  $\text{Ca}^{2+}$  content of the K4 core has a fairly uniform background level of 5 wt.%, with values of 15-20 wt.% occurring in the concretionary layer (Middelburg, 1990). The diagenetic model presented here indicates that steady state cementation would produce about 2 wt.%  $\text{Ca}^{2+}$ . It is unclear how much of the background  $\text{Ca}^{2+}$  is dolomitic cement but agreement for the steady state is close enough to the observed values to support the suggestion of Middelburg et al (1990) that there must be an important role for non-steady state diagenesis at the concretionary horizon. Numerous authors have suggested that the development of concretionary horizons is controlled by a pause in deposition. For example the calcitic concretions within Westphalian black shales of northern England (e.g. Curtis et al., 1986) may owe their origin to extremely slow rates of sedimentation ( $\sim 0.001 \text{ cm yr}^{-1}$ ) in waters with a high primary productivity (Fisher and Wignall, 2001). Larger masses of cement would clearly result during a pause in deposition which allows additional time for increased supply by diffusion and advection.

The steady state diagenetic models used here predict the extent of cementation from sulphate reduction that produces dispersed carbonate. However concretionary growth represents localised cementation, which could result by transport of  $\text{Ca}^{2+}$  removed from a large sediment volume and concentrated at a single site. The concentration of cement from a volume 500-1000 times larger than the volume of a spherical concretion requires that the radius of a spherical supply zone is 8-10x larger than the radius of the concretion. Thus a concretion of radius 20 cm would need to be 1.5-2 m away from the spherical supply zone of an adjacent concretion. These separations are significantly larger than those observed for Jet Rock (Upper Jurassic, UK) concretions (Raiswell and White, 1978; Raiswell, 1988b) which have a mean radius of 18 cm, and a mean nearest neighbour distance of 47 cm (suggesting a mean spherical supply zone of 24 cm radius). These data indicate an approximate 2.4:1 volume ratio of source sediment to concretion, which would allow the steady state cement concentrations to produce approximately 3.5 wt.% calcite or 7 wt. % dolomite by the concentration of cement at the concretion site. Higher volume ratios of source sediment to concretion could occur as burial depth increases, and the potential source sediment volume is extended vertically.

The steady state diagenetic models indicate that concretionary growth occurs in two stages; a first stage involves the transport-controlled precipitation of cement over shallow burial depths (driven by sulphate reduction), and a second stage involves slow growth possibly over substantial burial depths (Middelburg et al., 1990; Raiswell and Fisher, 2000). The first stage produces only small masses of cement but creates a framework which preserves local porosity and which is infilled over greater depths during the second stage.

A second stage of prolonged growth would indicate that a concretion should incorporate isotopic and chemical properties from several different depth-related processes in their cement compositions. This may include the continued addition of cement derived from the alkalinity generated during sulphate reduction, even though sulphate reduction has ceased (or is only occurring very slowly). Raiswell and Fisher (2000) argue that precisely this type of cementation (therein termed 'pervasive') is required to produce the typical isotopic and mineralogical variations found in concretionary cements. Raiswell et al. (2002) have shown that the earliest septarian cements inside Carboniferous concretions have  $\delta^{13}\text{C} = -28.7 \text{ ‰}$  and  $\delta^{18}\text{O} = -1.6 \text{ ‰}$ , which represent one end-member (derived from sulphate reduction) of a linear trend towards the last septarian cements ( $\delta^{13}\text{C} = -6.9 \text{ ‰}$  and  $\delta^{18}\text{O} = -14.6 \text{ ‰}$ ). By contrast the concretion cement ( $\delta^{13}\text{C} = -10$  to  $-12 \text{ ‰}$  and  $\delta^{18}\text{O} = -5.6$  to  $5.7 \text{ ‰}$ ) has an isotopic composition which suggests an origin after the earliest septaria. However the concretion cement cannot have completely post-dated the septaria, and must thus reflect some mixture of both the early and late septarian end-member cements.

## Conclusions

First order rate constants for  $\text{Ca}^{2+}$  removal during sulphate reduction can be estimated from porewater profiles showing decreasing concentrations of  $\text{Ca}^{2+}$  over depths of 15-150 m in DSDP/ODP sediments. In these sediments, rate constants vary from  $10^{-14}$  to  $10^{-11} \text{ s}^{-1}$  and are related to sedimentation rate such that  $\log k = 1.16 \log \omega - 10.3$ , indicating that faster rates of  $\text{Ca}^{2+}$  removal occur at the highest sedimentation rates. Faster sedimentation rates also produce higher degrees of saturation with respect to both calcite and dolomite, up to sedimentation rates of approximately  $0.1 \text{ cm yr}^{-1}$ .

Regardless of these relationships, the integrated masses of  $\text{Ca}^{2+}$  removed during sulphate reduction over these depths are always less than  $100 \text{ } \mu\text{mol cm}^{-2}$  and are sufficient to produce less than 1.5 wt% calcite or 3 wt. % dolomite in the compacted sediment. These concentrations are

inadequate to explain the occurrence of carbonate concretions with isotopically light  $\delta^{13}\text{C}$  compositions (indicating that carbonate was mainly derived from sulphate reduction). The growth of such concretions must therefore require some combination of:-

- (i) Diagenetic conditions that produce faster rates of sulphate reduction.
- (ii) More time for the formation of carbonate cement during sulphate reduction, for example as a result of a depositional hiatus.
- (iii) An alternative source of  $\text{Ca}^{2+}$  (such as dissolution of skeletal material) and a mechanism by which isotopically light carbonate (similar to that derived by sulphate reduction) can be supplied during deeper burial.

### **Acknowledgements**

The authors are pleased to thank John Morse and an anonymous referee for their critical but valuable comments.

## References

- Arvidson, R.S., Mackenzie, F.T., 1999. The dolomite problem: Control of precipitation kinetics by temperature and saturation state. *Am. J. Sci.*, 298, 257-298.
- Baker, P. A., Kastner, M., 1981. Constraints on the formation of sedimentary dolomite. *Science*, 213, 214-216.
- Baker, P.A., Burns, S., 1985. Occurrence and formation of dolomite in organic-rich continental margin sediments. *Am. Assoc. Petrol. Geol. Bull.*, 69, 1917-1930.
- Ben-Yaakov, S., 1973. pH buffering of pore water of Recent anoxic marine sediments. *Limnol. Oceanogr.*, 18, 86-94.
- Berner, R. A., 1975. The role of magnesium in the crystal growth of calcite and aragonite from seawater. *Geochim. Cosmochim. Acta*, 39, 489-504.
- Berner, R. A., 1980. *Early Diagenesis: A Theoretical Approach*. Princeton University Press, Princeton, N.J., 241p.
- Berner, R. A., Morse, J.W., 1974. The dissolution kinetics of calcium carbonate in seawater. IV: Theory of calcite dissolution. *Am. J. Sci.*, 274, 108-135.
- Boudreau, B.P., 1996. *Diagenetic Models and their Interpretation*. Springer-Verlag, Berlin, 414p.
- Boudreau, B.P., Canfield, D.E., 1993. A comparison of closed-system and open-system models for porewater pH and calcite saturation state. *Geochim. Cosmochim. Acta*, 57, 317-334.
- Boetius, A., Ravensschlag, K., Schubert, C.J., Rickett, D., Widdel, F., Gieske, A., Amann, R., Jorgensen, B.B., Witte, U., Pfannkuche, O., 2000. A marine microbial consortium apparently mediating anaerobic oxidation of methane. *Nature*, 407, 623-626.
- Buffle, J., De Vitre, R.R., Perret, D., Leppard, G.G., 1989. Physico-chemical characteristics of a colloidal iron phosphate species formed at the oxic-anoxic interface of a eutrophic lake. *Geochim. Cosmochim. Acta*, 53, 399-408.
- Burton, E.A., Walter, L.M., 1987. Relative precipitation rates of aragonite and Mg calcite from seawater: Temperature or carbonate ion control? *Geology*, 15, 111-114.
- Canfield, D.E., Raiswell, R., 1991. Carbonate precipitation and dissolution. In: Allison P.S.A., Briggs, D.E.G., (Eds.), *Taphonomy: Releasing the Data Locked in the Fossil Record*, Plenum Press, New York, pp. 411-453.
- Canfield, D.E., Thamdrup, B., Hansen, J.W., 1993. The anaerobic degradation of organic matter in Danish coastal sediments: Iron reduction, manganese reduction, and sulfate reduction. *Geochim. Cosmochim. Acta*, 57, 3867-3883.

- Claypool, G.E., Kaplan, I.R. 1974. The origin and distribution of methane in marine sediments. In: Kaplan, I.R. (Ed.), *Natural Gases in Marine Sediments*, Plenum, New York, pp. 97-139.
- Compton, J.S., 1988. Degree of supersaturation and precipitation of organogenic dolomite. *Geology*, 16, 318-321.
- Curtis, C.D., Coleman, M.L., Love, L.G., 1986, Pore water evolution during sediment burial from isotopic and mineral chemistry of calcite, dolomite and siderite concretions: *Geochim. Cosmochim. Acta*, v. 50, p. 2321-2334.
- Devol, A.H., 1983. Methane oxidation rates in the anaerobic sediments of Saanich Inlet. *Limnol. Oceanogr.*, 28, 738-742.
- Devol, A.H., Ahmed, S.I., 1983. Are higher rates of sulphate reduction associated with anaerobic methane oxidation? *Nature*, 291, 407-408.
- Drever, J.I., 1974. The magnesium problem. In: Goldberg, E.D., (Ed.), *The Sea*. Wiley-Interscience, New York, 5, 337-357.
- Fisher, Q.J., Wignall, P.B., 2001. Palaeoenvironmental controls on the uranium distribution in an Upper Carboniferous black shale (G. listeri Marine Band). *Chem. Geol.*, 175, 605-621.
- Froelich, P.N., Klinkhammer, G.P., Bender, M.L., Luedtke, N.A., Heath, G.R., Cullen, D., Dauphin, P., Hammond, D, Hartman, B., Maynard, V., 1979. Early oxidation of organic matter in pelagic sediments of the eastern equatorial Atlantic: Suboxic diagenesis. *Geochim. Cosmochim. Acta*, 43, 1075-1090.
- Gieskes, J.M., 1974. Interstitial water studies, Leg 25. In: Simpson E.W.S, Schlick, R., Gieskes, J.M., Arch Girdley, W., Leclaire, L., Marshall, B.V., Moore, C., Miller, C., Sigai, J., Vallier, T.L., White, S.M., Zobel, B., (Eds.), *Initial Reports of the Deep Sea Drilling Project*, XXV, 361-394.
- Gieskes, J.M., 1983. The chemistry of interstitial waters of deep-sea sediments: Interpretation of Deep Sea drilling data. In: Riley, J.P., Chester, R., (Eds.), *Chemical Oceanography*. Academic Press, London, 8, 221-269.
- Hardie, L.A., 1987. Dolomitization: A critical review of some current views. *J. Sedim. Petrol.*, 57, 66-183.
- Iverson, N., Jorgensen, B.B., 1985. Anaerobic methane oxidation rates at the sulfate-methane transition in marine sediments from Kattegat and Skagerrak (Denmark). *Limnol. Oceanogr.*, 30, 944-955.

- Kharaka, Y.K., Barnes, I., 1973. SOLMINEQ. Solution-mineral equilibria calculations. US Geological Survey Computer Contributions, NTIS PB-215 899.
- Luff, R., Wallmann, K., 2003. Fluid flow, methane fluxes, carbonate precipitation and biogeochemical turnover in gas hydrate-bearing sediments at Hydrate Ridge, Cascadia Margin: Numerical modelling and mass balances. *Geochim. Cosmochim. Acta*, 67, 3403-3421.
- Middelburg, J.J., 1990, PhD thesis. Early diagenesis and authigenic mineral formation in anoxic sediments of Kau Bay, Indonesia. Rijksuniversiteit Utrecht, 177p.
- Middelburg, J.J., de Lange, G.J., Krelen, R., 1990. Dolomite formation in anoxic sediments of Kau Bay, Indonesia. *Geology*, 18, 399-402.
- Morrow, W., Ricketts, B.D., 1986. Chemical controls on the precipitation of mineral analogues of dolomite: The sulfate enigma. *Geology*, 14, 408-410.
- Morse, J.W., 1983. The carbonate chemistry of North Atlantic Ocean deep-sea sediment pore water. In: Andersen, N.R., Malahoff, A. (Eds.), *The Fate of Fossil Fuel CO<sub>2</sub> in the Oceans*. Plenum, New York, p. 323-343.
- Morse, J.W., Mackenzie, F.T., 1990. *Geochemistry of Sedimentary Carbonates*, Developments in Sedimentology 48, Elsevier, Amsterdam, 707p.
- Morse, J.W., Arvidson, R.S., 2002. The dissolution kinetics of major sedimentary carbonate minerals. *Earth-Sci. Rev.*, 58, 51-84.
- Mozley, P.S., Burns, S.J., 1993. Oxygen and carbon isotopic composition of marine carbonate concretions: An overview. *J. Sedim. Petrol.*, 63, 73-83.
- Mucci, A., 1986. Growth kinetics and composition of magnesian calcite overgrowths precipitated from seawater: Quantitative influence of orthophosphate ions. *Geochim. Cosmochim. Acta*, 50, 2255-2265.
- Mucci, A., Morse, J.W., 1983. The incorporation of Mg<sup>2+</sup> and Sr<sup>2+</sup> into calcite overgrowths: Influences of growth rate and solution composition. *Geochim. Cosmochim. Acta*, 47, 217-233.
- Mucci, A., Canuel, R., Zhong, S., 1989. The solubility of calcite and aragonite in sulfate-free seawater and the seeded growth kinetics and composition of the precipitates at 25°C. *Chem. Geol.*, 74, 309-320.
- Naehr, T.H., Rodriguez, N.M., Bohrmann, G., Paull, C.K., Botz, R., 2000. Methane-derived authigenic carbonates associated with gas hydrate decomposition and fluid venting above the Blake Ridge diapir. In: Paull, C.K., Matsumoto, R., Wallace, P.J., Dillon, W.P., (Eds.). *Proc. ODP Sci. Results 164*, College station TX (Ocean Drilling Program), pp.285-300.

- Raiswell, R., 1976. The microbiological formation of carbonate concretions in the Upper Lias of NE England. *Chem. Geol.*, 18, 227-244.
- Raiswell, R., 1987. Non-steady state microbiological diagenesis and the origin of concretions and nodular limestones. In: Marshall, J.D. , (Ed.), *Diagenesis of Sedimentary Sequences*. Geol. Soc. London Spec. Publ., 36, 41-54.
- Raiswell, R., 1988a. Chemical model for the origin of limestone-shale cycles by anaerobic methane oxidation. *Geology*, 16, 641-644.
- Raiswell, R., 1988b. Evidence of surface reaction controlled growth of carbonate concretions in shales. *Sedimentology*, 35, 571-575.
- Raiswell, R., White, N.J.M., 1978. Spatial aspects of concretionary growth in the Upper Lias of N.E. England. *Sediment. Geol.*, 20, 291-300.
- Raiswell, R., Fisher, Q.J., 2000. Mudrock-hosted carbonate concretions: a review of growth mechanisms and their influence on chemical and isotopic composition. *J. Geol. Soc. London*, 157, 239-251.
- Raiswell, R., Bottrell, S.H., Dean, S.P., Marshall, J.D., Carr, A., Hatfield, D., 2002. Isotopic constraints on growth conditions of multiphase calcite-pyrite-barite concretions in Carboniferous mudstones. *Sedimentology*, 49, 237-254.
- Rodriguez, N.M., Paull, C.K., Borowski, W.S., 2000. Zonation of carbonates within gas hydrate-bearing sedimentary sections on the Blake Ridge: Offshore Southeastern North America. In: Paull, C.K., Matsumoto, R., Wallace, P.J., Dillon, W.P., (Eds.). *Proc. ODP Sci. Results 164*, College station TX (Ocean Drilling Program), pp.301-312.
- Russell, K.L., 1970. Geochemistry and halmyrolysis of clay minerals, Rio Ameca, Mexico. *Geochim. Cosmochim Acta*, 34, 893-907.
- Ruttenberg, K.C., Berner, R.A., 1993. Authigenic apatite formation and burial in Sediments from non-upwelling continental margin environments. *Geochim. Cosmochim. Acta*, 57, 991-1007.
- Savrda, C.E., Bottjer, D.J., 1988. Limestone concretion growth documented by trace fossils. *Geology*, 16, 908-911.
- Thamdrup, B., 2000. Bacterial manganese and iron reduction in aquatic sediments. *Advances in Microbial Ecology*. Schink, B. (Ed.), Kluwer, New York, pp.41-84.
- Thamdrup, B. Canfield, D.E., 1996. Pathways of carbon oxidation in continental margin sediments off central Chile. *Limnol. Oceanogr.*, 41, 1629-1650.

- Toth, D.I., Lerman, A., 1977. Organic matter reactivity and sedimentation rates in the ocean. *Am. J. Sci.*, 277, 265-285.
- Tromp. T.K., Van Cappellen, P., Key, R.M., 1995. A global model for early diagenesis of organic carbon and organic phosphorus in marine sediments. *Geochim. Cosmochim. Acta*, 59, 1259-1284.
- Ullman, W.J., Aller., R.C., 1982. Diffusion coefficients in nearshore marine sediments. *Limnol. Oceanogr.*, 27, 552-556.
- Van Cappellen, P., Berner, R.A., 1991. Fluorapatite crystal growth from modified seawater solutions. *Geochim. Cosmochim. Acta*, 55,1219. 1234.
- Van Cappellen, P., Berner,R.A., 1988. A mathematical model for the early diagenesis of phosphorus and fluorine in marine sediments: Apatite precipitation. *Am. J. Sci.*, 288, 289-333.
- Walter, L.M., 1986. Relative efficiency of carbonate dissolution and precipitation during diagenesis: A progress report on the role of solution chemistry. *J. Sedim. Petrol.*, 56, 1-11.
- Zhong, S., Mucci, A., 1993. Calcite precipitation from seawater using a constant addition technique: A new overall kinetic expression. *Geochim. Cosmochim. Acta*, 57, 1409-1417.

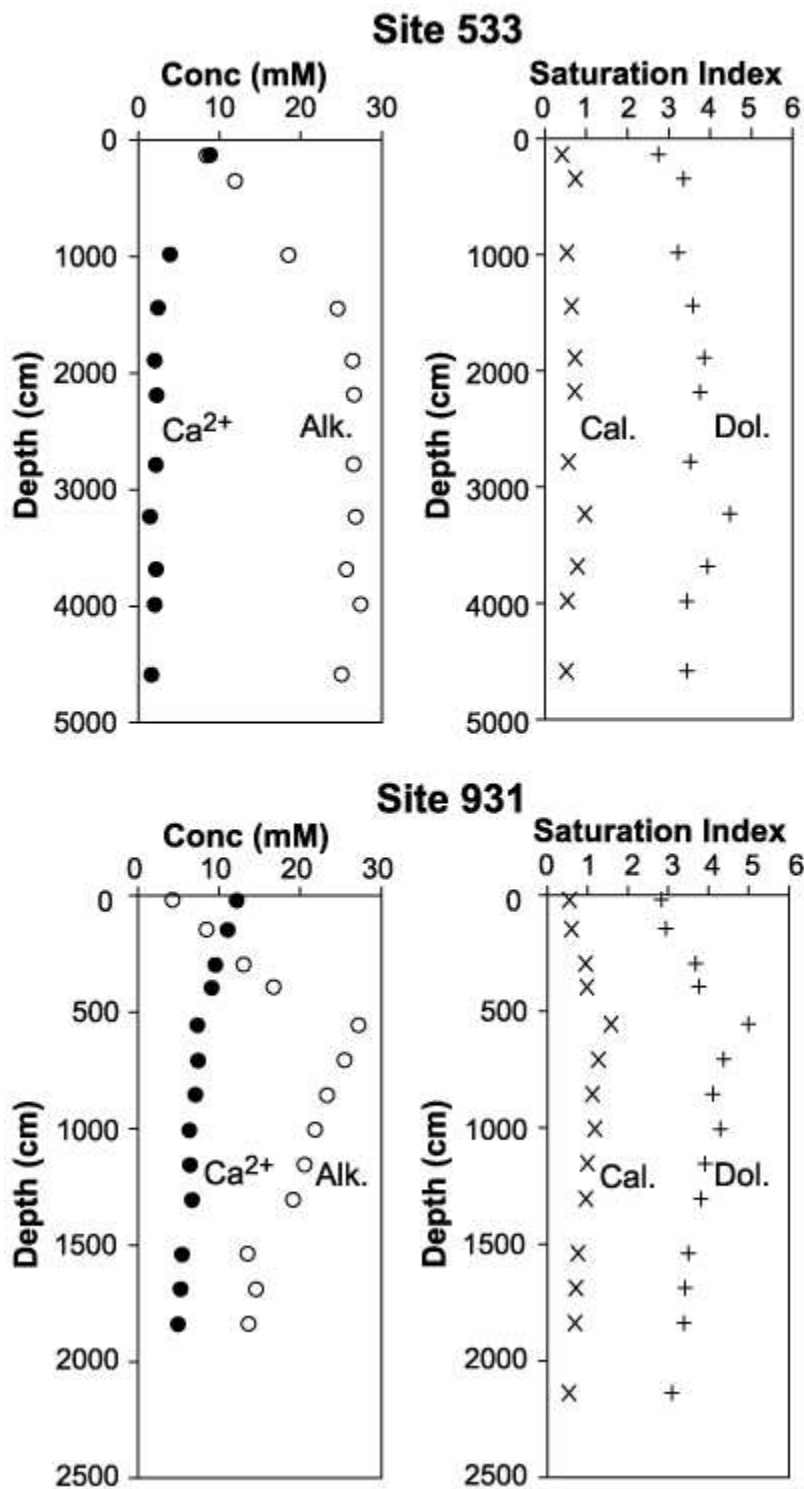


**Figure 1.** Chemical properties of porewaters at site 533 and 931. Filled circles are concentrations of  $\text{Ca}^{2+}$  and open circles are alkalinity, Crosses (X) are SI values for calcite and pluses (+) are SI values for dolomite.

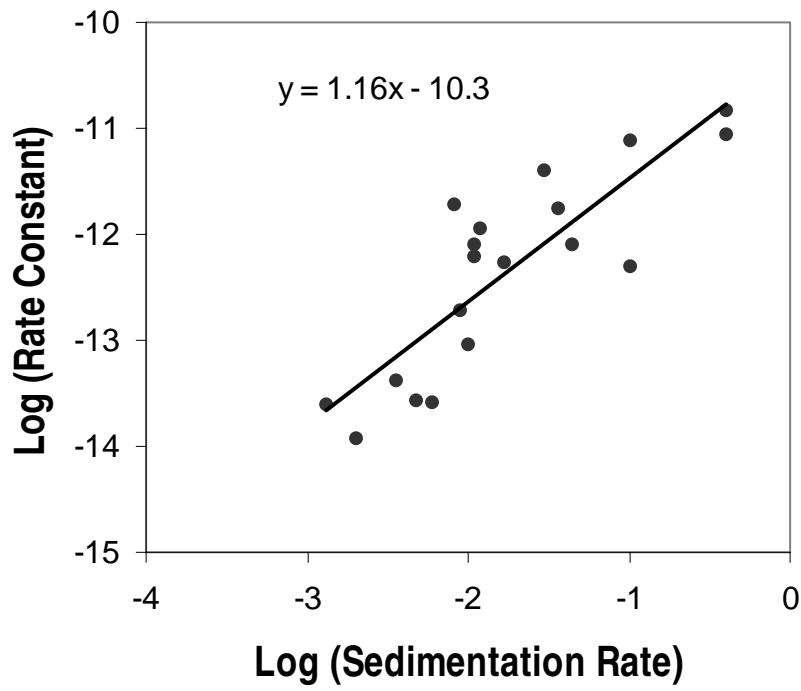


**Figure 2.** Variation in log Rate Constant ( $k$ ) with log Sedimentation Rate ( $\omega$ ) for DSDP/ODP sediments (Table 1)

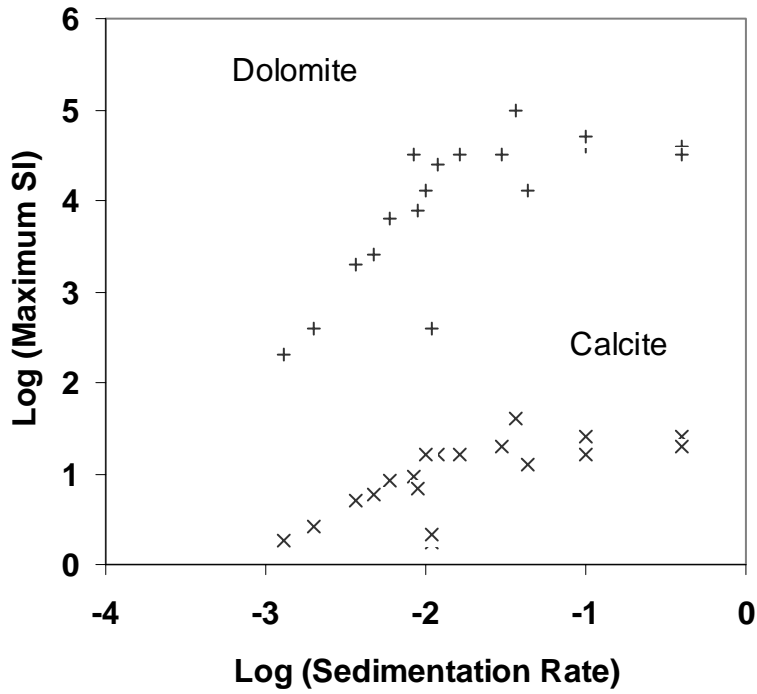


**Figure 3.** Variation in maximum Saturation Index (SI) values for calcite (X) and dolomite (+) with log Sedimentation Rate for DSDP/ODP sediments

**Table 1** Physical Characteristics of the Sample Sites

| Site | Water Depth (m) | Locality                      | Lithology                                     | Bottom Water Temp (°C) | Sed. Rate (cm yr <sup>-1</sup> ) |
|------|-----------------|-------------------------------|---|------------------------|----------------------------------|
| 478  | 1899            | Guaymas Basin                 | Diatomaceous muds, silty turbidites           | 3.4                    | 0.1                              |
| 481  | 1998            | Guaymas Basin                 | Diatomaceous muds, muddy sands                | 3.6                    | 0.1                              |
| 533  | 3191            | Blake Outer Ridge             | Burrowed nannofossil silty marls and clays    | 2.4                    | 0.0083                           |
| 565  | 3099            | Middle America Trench         | Uniform, massive, mud and mudstone            | 2.0                    | 0.0165                           |
| 572A | 3893            | Central Equatorial Pacific    | Siliceous nannofossil chalks, oozes           | 2.5                    | 0.0013                           |
| 721A | 1945            | W. Arabian Sea                | Nannofossil chalks and oozes                  | 1.8                    | 0.0048                           |
| 722A | 2028            | W. Arabian Sea                | Foraminifera-bearing chalks and oozes         | 2.5                    | 0.0036                           |
| 763A | 1368            | Central Exmouth Plateau       | Nannofossil ooze with foraminifera            | 4.0                    | 0.002                            |
| 798B | 900             | Oki Ridge, Sea of Japan       | Diatomaceous clays and silts                  | 2.0                    | 0.012                            |
| 819A | 577             | Great Barrier Reef            | Clay and carbonate-rich pteropod ooze         | 10.0                   | 0.011                            |
| 821A | 213             | Great Barrier Reef            | Calcareous silts and clays                    | 10.0                   | 0.01                             |
| 823A | 1639            | W. Queensland Trough          | Nannofossil ooze with micrite.                | 4.0                    | 0.011                            |
| 908A | 1285            | Hovgaard Ridge, Boreas Basin  | Clayey and silty mud                          | -0.5                   | 0.006                            |
| 911A | 902             | Yermak Plateau, Greenland Sea | Bioturbated silty clay and clayey silt        | -0.3                   | 0.009                            |
| 931B | 3475            | SE. margin, Amazon Fan        | Bioturbated nannofossil and foraminifera clay | 2.4                    | 0.036                            |
| 939B | 2792            | E. flank, Amazon              | Burrowed foraminifera-nannofossil clay        | 2.8                    | 0.40                             |

|      |      |                             |   |     |       |
|------|------|-----------------------------|---|-----|-------|
|      |      | Channel                     |   |     |       |
| 939C | 2791 | E. flank, Amazon<br>Channel | Burrowed foraminifera-nannofossil clay    | 2.8 | 0.40  |
| 942A | 3348 | W. edge, Amazon<br>Fan      | Bioturbated nannofossil foraminifera clay | 2.6 | 0.044 |
| 944D | 3709 | Middle Amazon<br>Fan        | Bioturbated nannofossil foraminifera clay | 2.4 | 0.03  |

**Table 2.** Model boundaries and parameters.

| Site | Porosity | Upper Depth (cm) | Lower Depth (cm) | Exponent (B)           | r    | Rate Constant (k in s <sup>-1</sup> ) | ΣR (μmol cm <sup>-2</sup> ) | Range SI <sub>cal</sub> | Range SI <sub>dol</sub> |
|------|----------|------------------|------------------|------------------------|------|---------------------------------------|-----------------------------|-------------------------|-------------------------|
| 478  | 0.83     | 0                | 4800             | 5.8 x 10 <sup>-5</sup> | 0.91 | 5±25 x 10 <sup>-12</sup>              | 23±115                      | 0.96-1.4                | 3.8-4.6                 |
| 481  | 0.88     | 0                | 1580             | 7.1 x 10 <sup>-4</sup> | 0.98 | 8±4 x 10 <sup>-12</sup>               | 31±17                       | 1.1-1.2                 | 4.5-4.7                 |
| 533  | 0.58     | 0                | 1888             | 9.0 x 10 <sup>-4</sup> | 0.99 | 1.9±0.5 x 10 <sup>-12</sup>           | 45±16                       | 0.42-0.97               | 2.8-4.5                 |
| 565  | 0.69     | 0                | 4640             | 2.8 x 10 <sup>-4</sup> | 0.88 | 5±2 x 10 <sup>-13</sup>               | 25±12                       | 0.68-1.2                | 3.2-4.5                 |
| 572D | 0.78     | 0                | 950              | 8.0 x 10 <sup>-5</sup> | 0.97 | 2.5±0.7 x 10 <sup>-14</sup>           | 63±24                       | 0.15-0.27               | 2.1-2.3                 |
| 721A | 0.63     | 0                | 5405             | 5.5 x 10 <sup>-5</sup> | 0.99 | 2±1 x 10 <sup>-14</sup>               | 22±12                       | 0.18-0.76               | 2.3-3.4                 |
| 722A | 0.65     | 0                | 5415             | 8.8 x 10 <sup>-5</sup> | 0.91 | 4±1 x 10 <sup>-14</sup>               | 25±9                        | 0.29-0.71               | 2.5-3.3                 |
| 763A | 0.70     | 290              | 4880             | 4.5 x 10 <sup>-5</sup> | 0.99 | 1.2±0.4 x 10 <sup>-14</sup>           | 32±12                       | 0.12-0.41               | 1.9-2.6                 |
| 798B | 0.72     | 0                | 1285             | 5.2 x 10 <sup>-4</sup> | 0.96 | 1.1±0.3 x 10 <sup>-12</sup>           | 43±16                       | 0.66-1.2                | 3.1-4.4                 |
| 819A | 0.58     | 0                | 2545             | 4.3 x 10 <sup>-4</sup> | 0.97 | 8±2x 10 <sup>-13</sup>                | 28±10                       | 0.17-0.25               | 2.3-2.6                 |
| 821A | 0.55     | 0                | 14480            | 9.3 x 10 <sup>-5</sup> | 0.96 | 10±6 x 10 <sup>-14</sup>              | 17±11                       | 0.46-1.2                | 1.9-4.1                 |
| 823A | 0.66     | 0                | 3225             | 3.7 x 10 <sup>-4</sup> | 0.96 | 6±2 x 10 <sup>-13</sup>               | 37±14                       | 0.14-0.32               | 2.1-2.6                 |
| 908A | 0.46     | 445              | 8880             | 4.9 x 10 <sup>-5</sup> | 0.94 | 3±4 x 10 <sup>-14</sup>               | 14±19                       | 0.37-0.93               | 2.6-3.8                 |
| 911A | 0.48     | 0                | 6295             | 2.0 x 10 <sup>-4</sup> | 0.93 | 2±1 x 10 <sup>-13</sup>               | 14±8                        | 0.69-0.84               | 3.0-3.9                 |
| 931B | 0.66     | 20               | 1838             | 4.6 x 10 <sup>-4</sup> | 0.96 | 2±1 x 10 <sup>-12</sup>               | 25±14                       | 0.41-1.6                | 2.8-5.0                 |
| 939B | 0.62     | 145              | 3045             | 2.6 x 10 <sup>-4</sup> | 0.98 | 2±11 x 10 <sup>-11</sup>              | 20±12                       | 0.84-1.4                | 3.7-4.6                 |
| 939C | 0.64     | 20               | 1650             | 4.3 x 10 <sup>-4</sup> | 0.98 | 3±13 x 10 <sup>-11</sup>              | 20±87                       | 0.50-1.3                | 2.7-4.5                 |
| 942A | 0.67     | 145              | 3525             | 2.0 x 10 <sup>-4</sup> | 0.99 | 8±8 x 10 <sup>-13</sup>               | 20±21                       | 0.84-1.1                | 3.4-4.1                 |
| 944D | 0.69     | 0                | 950              | 9.2 x 10 <sup>-4</sup> | 0.99 | 4±1 x 10 <sup>-12</sup>               | 34±12                       | 0.54-1.3                | 3.1-4.5                 |

The depth-integrated masses of Ca<sup>2+</sup> removed (ΣR) are expressed relative to volumes of porewater plus sediment.